Molecular packing and intermolecular interactions in N-acylethanolamines: Crystal structure of N-myristoylethanolamine

ARTICLE *in* BIOCHIMICA ET BIOPHYSICA ACTA · JUNE 1999

Impact Factor: 4.66 · DOI: 10.1016/S0005-2736(99)00035-8 · Source: PubMed

ELSEVIER

Biochimica et Biophysica Acta 1418 (1999) 261–267

BIOCHIMICA ET BIOPHYSICA ACTA
BBA

Molecular packing and intermolecular interactions in *N*-acylethanolamines: crystal structure of *N*-myristoylethanolamine

M. Ramakrishnan, Musti J. Swamy *

School of Chemistry, University of Hyderabad, Hyderabad 500 046, India

Received 1 December 1998; received in revised form 11 February 1999; accepted 22 February 1999

Abstract

N-Acylethanolamines elicited much interest in recent years owing to their occurrence in biological membranes under conditions of stress as well as under normal conditions. The molecular conformation, packing properties and intermolecular interactions of *N*-myristoylethanolamine (NMEA) have been determined by single crystal X-ray diffraction analysis. The lipid crystallized in the space group $P2_1/a$ with unit cell dimensions: $a = 9.001$, $b = 4.8761$, $c = 39.080$. There are four symmetry-related molecules in the monoclinic unit cell. The molecules are organized in a tail-to-tail fashion, similar to the arrangement in a bilayer membrane. The hydrophobic acyl chain of the NMEA molecule is tilted with respect to the bilayer normal by an angle of 37°. Each hydroxy group forms two hydrogen bonds, one as a donor and the other as an acceptor, with the hydroxy groups of molecules in the opposing leaflet. These O–H···O hydrogen bonds form an extended, zig-zag type network along the *b*-axis. In addition, the N–H and C=O groups of adjacent molecules are involved in N–H···O hydrogen bonds, which also connect adjacent molecules along the *b*-axis.

Keywords: *N*-Acylethanolamine; Crystal structure; X-ray diffraction; Lipid membrane; Conformation; Molecular packing; Hydrogen bonding

1. Introduction

N-Acylethanolamines (NAEs) and *N*-acylphosphatidylethanolamines (NAPEs) are naturally occurring amphiphilic molecules present in biological membranes [1]. Their content increases dramatically when the parent organisms are subjected to conditions of stress, such as injury in animals, or dehydration in plant seeds. Both NAEs and NAPEs have been shown to accumulate in mammalian tissues undergoing extensive degeneration involving phospholipid degradation, such as ischemic rat brain and infarcted canine myocardium [2–4]. A phospholipase D-type enzyme cleaves NAPE in vivo to generate NAE, which then acts as a second messenger [5]. NAEs exhibit interesting biological and medicinal properties (for reviews see [1,5]). Especially, it has been shown that *N*-arachidonylethanolamine (anandamide) acts as an endogenous ligand for cannabinoid receptor [6], reduces sperm fertilizing capacity [7] and inhibits gap junction conductance [8], whereas *N*-oleoylethanolamine is a potent inhibitor of ceramidase [9].

In addition to the NAEs with unsaturated acyl chains, as alluded to above, those with saturated acyl chains also exhibit interesting biological proper-

Abbreviations: NAE, *N*-acylethanolamine; NMEA, *N*-myristoylethanolamine; NAPE, *N*-acylphosphatidylethanolamine; PC, phosphatidylcholine; PE, phosphatidylethanolamine

* Corresponding author. Fax: +91 (40) 301-0120/0145; E-mail: mjssc@uohyd.ernet.in

0005-2736/99/$ – see front matter
PII: S0005-2736(99)00035-8

ties. In mast cells, for example, *N*-palmitoylethanolamine acts as an agonist for the cannabinoid receptor type-2 [10]. Very recently, Chapman and colleagues have shown that treatment of tobacco cells with a fungal elicitor, such as xylanase, results in the accumulation of *N*-lauroylethanolamine and *N*-myristoylethanolamine, which accumulate in the culture medium [11]. This observation has been interpreted as indicative of plant NAEs playing a role in a signaling pathway analogous to the one found in mammalian cells [5,11].

In addition to the interesting biological properties that they exhibit, NAEs and NAPEs are likely to be useful in developing liposomal formulations for drug delivery applications, since recent studies indicate that compounds belonging to these two classes stabilize the bilayer structure [12–14].

Considering the variety of interesting properties exhibited by NAEs and NAPEs described above, it is important to systematically investigate their properties in order to develop structure–function relationships to rationalize their functions. While a considerable amount of knowledge exists on the biological, medicinal and pharmacological properties of NAEs, as outlined above, relatively very little is known regarding their supramolecular structure both in the solid state as well as in solution, phase behavior and interaction with other membrane lipids. In order to fill this lacuna, we initiated a long-term program to investigate the phase behavior and structure of NAEs and NAPEs and their interaction with other membrane lipids. In earlier studies, we have investigated the chain-melting phase transitions of homologous series of these two classes of compounds by differential scanning calorimetry [15–17]. In the present study, the crystal structure of *N*-myristoylethanolamine is reported and the intermolecular interactions and the molecular packing in the crystal are analyzed.

2. Materials and methods

2.1. Materials

Myristic acid was purchased from Sigma (St. Louis, USA). Oxalyl chloride was from Merck (Darmstadt, Germany). Ethanolamine was obtained from Ranbaxy (Mumbai, India). Myristic acid was converted to myristoyl chloride by treating with 4 mol equivalents of oxalyl chloride according to the procedure described in [18]. *N*-Myristoylethanolamine was synthesized by the reaction of myristoyl chloride with ethanolamine and characterized by thin layer chromatography (TLC) and infrared (IR) spectroscopy as reported earlier [15]. All solvents were distilled and dried prior to use.

2.2. Crystallization and X-ray diffraction

Needle-shaped, colorless crystals of NMEA were grown at room temperature from a 1:1 mixture of dichloromethane and toluene, containing a trace of ethanol. A crystal of $0.2\times0.16\times0.4$ mm size was used for the data collection in the present study. X-ray diffraction measurements were carried out with an automated Enraf–Nonius Mach-3 diffractometer using graphite monochromater, Mo-Kα ($\lambda=0.71073$ Å) radiation. Intensity data were collected by ω-scan mode. Crystal stability was monitored by measuring the intensity of three standard reflections at 90-min intervals. No appreciable variation was detected.

2.3. Structure solution and refinement

The data collected in the range of $\theta=1.56$–$24.98°$ were reduced using the XTAL program [19]. Structure solution was carried out in the monoclinic space group. No absorption correction was applied. The structure was solved successfully by direct methods in the space group $P2_1/a$ and refined by full matrix least-squares procedure using the SHELXL97 program [20]. The refinement was carried out using 731 absorbed [$>4\sigma(F)$] reflections and converged to a final $R_1=6.02$, w$R_2=16.68$ and goodness of fit = 1.102. Carbon atoms in the hydrophobic region (C4–C16) were refined isotropically, whereas C1–C3 and the heteroatoms were refined anisotropically. Hydrogen atoms were included in the structure factor calculation with fixed thermal parameters at idealized positions, but were not refined.

2.4. Crystal parameters of NMEA

Molecular formula, $C_{16}H_{33}NO_2$; molecular weight, 271.44. Crystals were colorless and needle-shaped.

Crystal system, monoclinic; space group (Sg), $P2_1/a$. Unit cell dimensions (with standard deviations in parentheses): $a = 9.001$ (3); $b = 4.8761$ (19); $c = 39.08$ (10) Å; $\alpha = 90.0$; $\beta = 90.16$ (3); and $\gamma = 90.0$. Volume of the unit cell, $V = 1715.2$ (9) Å^3. Number of molecules in the unit cell, $Z = 4$. Angle of tilt (of the acyl chains), $\phi = 37°$. Cross-sectional area of the unit cell, $\Sigma = 43.89$ Å^2. Area per molecule, $S = 21.95$ Å^2.

3. Results and discussion

The interest in *N*-acylethanolamines has been growing dramatically over the past several years in view of their various interesting biological and medicinal properties [1,5]. In order to understand how the different effects are caused by NAEs, it is essential to investigate the properties of these molecules in a systematic manner. Particularly, studies aimed at understanding the phase behavior and structures formed by them in the solid state as well as in the fully hydrated state will be of immense value in understanding their biological implications in the parent organism. In view of this, in earlier studies we investigated the thermotropic phase behavior of a homologous series of NAEs of both even and odd number of C-atoms, using differential scanning calorimetry [15,16]. In the present communication, we report the crystal structure of *N*-myristoylethanolamine and discuss the packing properties and intermolecular interactions of this compound in the crystal lattice.

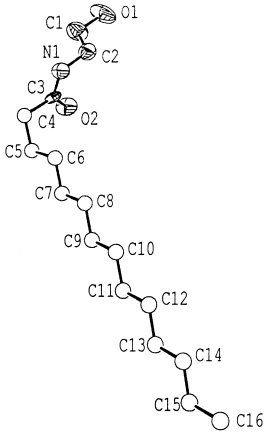

Fig. 1. ORTEP plot of *N*-myristoylethanolamine. The atom numbering is indicated in the figure. The hatched symbols indicate atoms that are refined anisotropically.

Table 1
Atomic coordinates ($\times 10^4$) and equivalent isotropic displacement parameters; (Å$^2 \times 10^3$) for *N*-myristoylethanolamine

Atom	*x*	*y*	*z*	*U*(eq)
N(1)	5697 (5)	3616 (9)	4023 (1)	58 (1)
O(2)	5329 (5)	8003 (8)	3873 (1)	72 (1)
O(1)	7247 (6)	5512 (10)	4864 (1)	107 (2)
C(1)	6111 (8)	4947 (16)	4611 (2)	87 (2)
C(2)	6819 (7)	4226 (12)	4285 (1)	68 (2)
C(3)	5047 (5)	5539 (10)	3838 (1)	41 (1)
C(4)	3919 (5)	4611 (11)	3576 (1)	50 (1)
C(5)	4239 (6)	5681 (12)	3217 (1)	53 (1)
C(6)	5629 (5)	4557 (11)	3055 (1)	50 (1)
C(7)	5907 (5)	5627 (11)	2699 (1)	52 (1)
C(8)	7239 (6)	4438 (12)	2519 (1)	50 (1)
C(9)	7501 (6)	5587 (11)	2166 (1)	52 (1)
C(10)	8827 (6)	4408 (12)	1981 (1)	53 (1)
C(11)	9079 (6)	5596 (11)	1626 (1)	53 (1)
C(12)	10409 (6)	4404 (12)	1440 (1)	54 (1)
C(13)	10632 (6)	5567 (12)	1087 (1)	58 (1)
C(14)	11958 (6)	4412 (12)	898 (1)	61 (2)
C(15)	12162 (7)	5591 (14)	541 (2)	71 (2)
C(16)	13520 (7)	4424 (16)	357 (2)	87 (2)

$$U(\text{eq}) = 1/3 \sum_i \sum_j U_{ij} a_i * a_j * a_i\, a_j \cos(ai, aj)$$

3.1. Description of the structure

An ORTEP plot describing the crystal structure of NMEA is shown in Fig. 1 along with the atom numbering for all the non-hydrogen atoms. The atomic coordinates and equivalent isotropic displacement parameters for the non-hydrogen atoms are given in Table 1. The bond distances, bond angles and torsion angles involving all the non-hydrogen atoms are given in Tables 2–4, respectively. As is clearly seen from Fig. 1, the hydrocarbon portion (C5–C16) of the acyl chain of the molecule is in all-*trans* conformation. The torsion angles observed for the acyl chain region, with the exception of the C3–C4–C5–C6 angle, which is 68.5°, are all in the neighborhood of 180° and are fully in agreement with the above observation. The gauche conformation at the C4–C5 bond results in a bending of the molecule, giving it an 'L' shape. The carbonyl group and the amide N–H are also in the *trans* geometry.

Table 2
Bond distances (Å) for *N*-myristoylethanolamine

N(1)–C(3)	1.321 (6)
N(1)–C(2)	1.466 (7)
O(2)–C(3)	1.236 (6)
O(1)–C(1)	1.446 (7)
C(1)–C(2)	1.471 (9)
C(3)–C(4)	1.508 (7)
C(4)–C(5)	1.523 (7)
C(5)–C(6)	1.508 (7)
C(6)–C(7)	1.506 (7)
C(7)–C(8)	1.509 (7)
C(8)–C(9)	1.508 (7)
C(9)–C(10)	1.511 (7)
C(10)–C(11)	1.519 (7)
C(11)–C(12)	1.518 (7)
C(12)–C(13)	1.507 (7)
C(13)–C(14)	1.515 (7)
C(14)–C(15)	1.518 (8)
C(15)–C(16)	1.530 (9)

Table 3
Bond angles (degrees) for *N*-myristoylethanolamine

C(3)–N(1)–C(2)	122.8 (5)
O(1)–C(1)–C(2)	109.3 (6)
N(1)–C(2)–C(1)	110.8 (5)
O(2)–C(3)–N(1)	122.5 (5)
O(2)–C(3)–C(4)	120.4 (5)
N(1)–C(3)–C(4)	117.0 (4)
C(3)–C(4)–C(5)	113.1 (4)
C(6)–C(5)–C(4)	115.0 (4)
C(5)–C(6)–C(7)	113.8 (4)
C(6)–C(7)–C(8)	115.6 (4)
C(7)–C(8)–C(9)	114.3 (4)
C(10)–C(9)–C(8)	115.0 (5)
C(9)–C(10)–C(11)	114.3 (5)
C(12)–C(11)–C(10)	114.3 (5)
C(13)–C(12)–C(11)	113.7 (5)
C(12)–C(13)–C(14)	114.5 (5)
C(15)–C(14)–C(13)	113.8 (5)
C(14)–C(15)–C(16)	112.9 (5)

3.2. Molecular packing

Packing diagrams of *N*-myristoylethanolamine along the *a*-axis and *b*-axis are given in Fig. 2A and B, respectively. The NMEA molecules are packed head-to-head (and tail-to-tail) in stacked bilayers. The O–H···O hydrogen bonds between the head groups of opposite leaflets of the bilayer are most likely the driving force for this arrangement (see below). In addition, the amide groups of adjacent molecules along the *b*-axis are also involved in hydrogen bonds. The carbonyl oxygen atoms of adjacent molecules point in the opposite direction, thus providing the appropriate juxtaposition of the amide carbonyl and hydrogen atoms to interconnect the adjacent molecules by hydrogen bonds. The methyl ends of the stacked bilayers are in van der Waals contacts, with the closest methyl–methyl contact distance (C16–C16) between the opposing layers being 4.13 Å. The distance between the methyl groups of adjacent molecules in the same layer is 5.79 Å.

The bilayer thickness (O1–O1 distance) for NMEA is 38.1 Å and the all-*trans* acyl chains are tilted by 37° with respect to the bilayer normal. This is similar to the arrangement found in long chain fatty acids and alcohols [21], which also pack in a bilayer form with tail-to-tail hydrocarbon chain alignment. However, it is different from arrangement found in lysolipids, such as lyso PC [22], which pack in an interdigitated mode resulting in two hydrocarbon chains being accommodated per polar group. Thus the thickness of the hydrophobic region of the bilayer is equal to the sum of the projected lengths of two acyl chains, whereas the thickness of the hydrophobic portion in lysolipids corresponds to that of the hydrocarbon region of one fatty acid

Table 4
Torsion angles (degrees) for *N*-myristoylethanolamine

C(3)	N(1)	C(2)	C(1)	85.1 (8)
C(2)	N(1)	C(3)	O(2)	1.0 (10)
C(2)	N(1)	C(3)	C(4)	177.9 (6)
O(1)	C(1)	C(2)	N(1)	177.4 (6)
O(2)	C(3)	C(4)	C(5)	51.0 (8)
N(1)	C(3)	C(4)	C(5)	−126.0 (6)
C(3)	C(4)	C(5)	C(6)	68.5 (7)
C(4)	C(5)	C(6)	C(7)	177.7 (5)
C(5)	C(6)	C(7)	C(8)	−176.1 (5)
C(6)	C(7)	C(8)	C(9)	−178.4 (6)
C(7)	C(8)	C(9)	C(10)	−179.6 (6)
C(8)	C(9)	C(10)	C(11)	179.9 (8)
C(9)	C(10)	C(11)	C(12)	179.6 (5)
C(10)	C(11)	C(12)	C(13)	179.3 (5)
C(11)	C(12)	C(13)	C(14)	179.7 (6)
C(12)	C(13)	C(14)	C(15)	178.9 (6)
C(13)	C(14)	C(15)	C(16)	178.9 (7)

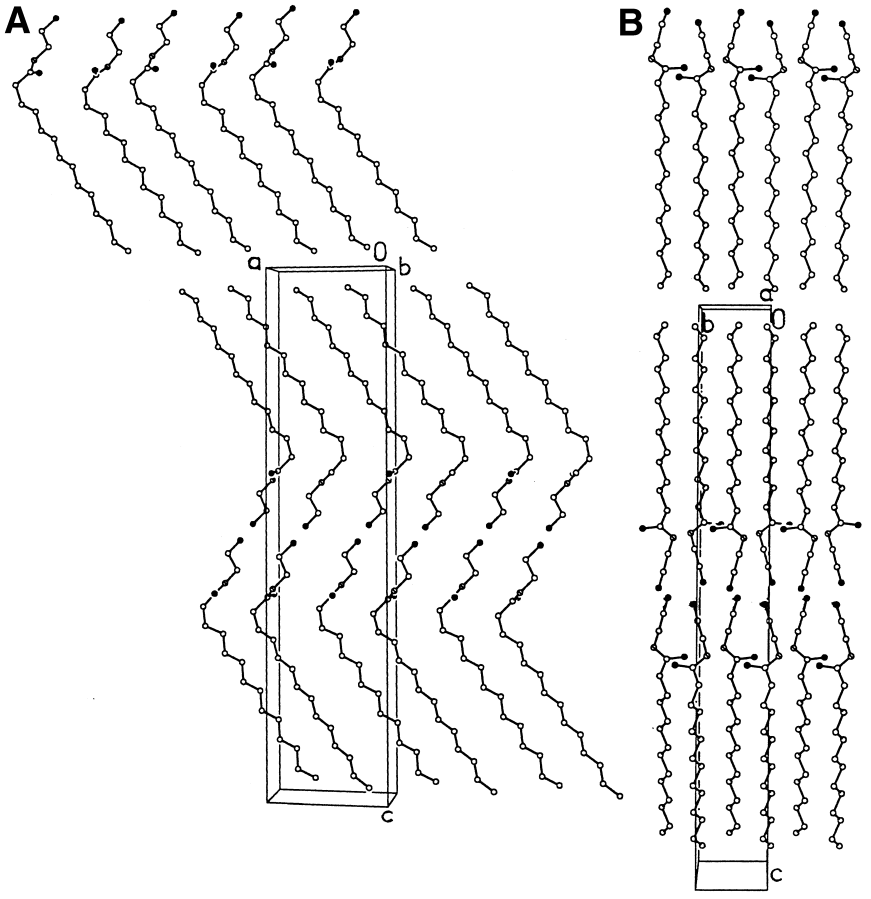

Fig. 2. Packing diagrams of *N*-myristoylethanolamine. (A) View along the *a*-axis. (B) View along the *b*-axis.

only. The tilted hydrocarbon chain arrangement is consistent with the alternation observed in the thermodynamic parameters between the homologous series of NAEs containing even and odd chain lengths [16].

3.3. Molecular area

The area per each NMEA molecule in the bilayer plane is 21.95 $Å^2$ and is in the same range as that found for 3(11-bromoundecanoyl)-D-glycerol, 3-lauroyl-D-glycerol, and 3-stearoyl-D-glycerol which have the molecular areas in the range of 21.5–22.7 $Å^2$ [23–26]. Other single chain lipids, such as lysophosphatidic acid and lysophosphatidylethanolamine, have somewhat larger molecular areas (33.6 and 34.8 $Å^2$, respectively) [26–28]. In the case of these two molecules, the very high tilt angle results in such large areas per molecule.

3.4. Hydrogen bonding and intermolecular interactions

To understand the intermolecular interactions, in the crystal structure of NMEA, the molecular packing in the crystal was examined from various angles. The hydrogen bonding pattern observed in the crystal lattice of NMEA is depicted in Fig. 3. Fig. 3A gives a picture of the molecular packing together with the hydrogen bonds between the hydroxyl groups in opposite leaflets as well as those between the amide N–H and carbonyl oxygen in adjacent layers in the same side of the bilayer. A closer picture of the hydrogen bonding pattern is given in Fig. 3B which gives the view along the *b*-axis. Each hydroxy group is involved in two hydrogen bonds, one as a hydrogen bond donor and the other as a hydrogen bond acceptor. All these hydrogen bonds connect the NMEA molecules only along the *b*-axis. Thus, in the

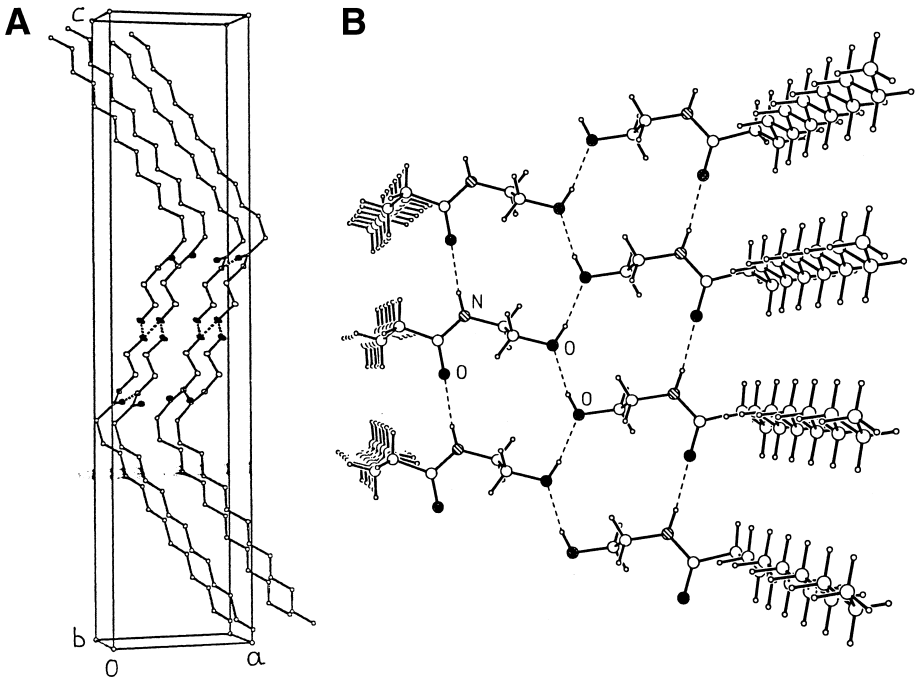

Fig. 3. Hydrogen bonding pattern in the crystal lattice of *N*-myristoylethanolamine. (A) A view of the bilayer displaying both the O–H···O and N–H···O type hydrogen bonds. (B) A close-up view along the *b*-axis. The hydrogen bonds are indicated by dashed lines. small open circles, hydrogen; large open circles, carbon; closed circles, oxygen; hatched circles, nitrogen.

unit cell containing four NMEA molecules in a bilayer form, the hydroxy group of each molecule forms one hydrogen bond within the same unit cell, whereas one more hydrogen bond is formed with another molecule from one of the adjacent unit cells along the *b*-axis. All the O–H···O hydrogen bonds in *N*-myristoylethanolamine have the same H···O distance of 1.89 Å and the distance between the two oxygen atoms is 2.7 Å. These hydrogen bonds are non-linear with the angle between the covalent bond and the hydrogen bond being 159.2°.

In addition to the hydrogen bonds between the hydroxy groups, there are also strong hydrogen bonds between the amide N–H and carbonyl oxygen of adjacent NMEA molecules along the *b*-axis. The distance between hydrogen bonded carbonyl oxygen and the amide hydrogen atom is 1.97 Å and the N···O distance is 2.82 Å. The angle between the covalent bond and the hydrogen bond (N–H···O angle) is 166.7°.

From Fig. 3, it is clear that the O–H···O hydrogen bonds form extended networks along the *b*-axis, which stabilize the bilayer arrangement in the crystal lattice. The network has a zig-zag arrangement, with the angle between the two hydrogen bonds (O1–O1–O1 angle) at each oxygen atom being 129.4°. The N–H···O hydrogen bonds connect adjacent NMEA molecules in the same plane along the *b*-axis. Thus while the N–H group of each NMEA molecule forms a hydrogen bond with another molecule in the adjacent unit cell on one side, the carbonyl oxygen atom from the same molecule is involved in another hydrogen bond with the amide N–H of an NMEA molecule in the unit cell on the other side (Fig. 3B).

Ambrosini et al. [14] investigated the effect of two NAEs, namely, *N*-lauroylethanolamine and *N*-oleylethanolamine on the phase behavior of egg phosphatidylethanolamine and suggested that the NAEs may stabilize the bilayer structure. The results of the present study indicate that such stabilization is probably driven by the strong tendency of the NAEs to form bilayer structure. Considering that intermolecular hydrogen bonds between the head groups of neighboring molecules are found in crystal structures of PE [28] as well as NAE (present study), it is possible that hydrogen bond formation between the PE and NAE may play a role in such stabilization. Detailed studies on the interaction between these two

classes of lipids are required in order to understand the intermolecular interactions between them.

4. Conclusions

The first crystal structure of an *N*-acylethanolamine, namely *N*-myristoylethanolamine has been solved by single crystal X-ray diffraction. The structure clearly demonstrates that the NAE molecules adopt a bilayer-type arrangement with tail-to-tail chain packing. This arrangement is stabilized by intermolecular hydrogen bonds between the hydroxy groups of NMEA molecules in opposite leaflets as well as between the amide N–H and carbonyl oxygen of adjacent molecules in the same leaflet. Further stabilization is provided by the van der Waals' forces between the acyl chains. These results give a structural explanation for the bilayer stabilizing property exhibited by *N*-acylethanolamines when used in mixtures with phospholipids, such as phosphatidylethanolamine, which have the propensity to form non-bilayer structures.

Acknowledgements

This work was supported by a research grant from the Department of Science and Technology to M.J.S. The Enraf–Nonius Mach-3 single-crystal X-ray diffractometer, used in this study, was funded by the Department of Science and Technology, Government of India. The authors are grateful to Dr. Samudranil Pal for his help and advice in the X-ray data collection and analysis.

References

[1] H.H.O. Schmid, P.C. Schmid, V. Natarajan, Prog. Lipid Res. 29 (1990) 1–43.
[2] D.E. Epps, V. Natarajan, P.C. Schmid, H.H.O. Schmid, Biochim. Biophys. Acta 618 (1980) 420–430.
[3] D.E. Epps, F. Mandel, A. Schwartz, Cell Calcium 3 (1982) 531–543.
[4] V. Natarajan, P.C. Schmid, H.H.O. Schmid, Biochim. Biophys. Acta 878 (1986) 32–41.
[5] H.H.O. Schmid, P.C. Schmid, V. Natarajan, Chem. Phys. Lipids 80 (1996) 133–142.
[6] W.A. Devane, L. Hanus, A. Breuer, R.G. Pertwee, L.A. Stevenson, G. Griffin, D. Gibson, A. Mandelbaum, A. Etinger, R. Mechoulam, Science 258 (1992) 1946–1949.
[7] H. Schuel, E. Goldstein, R. Mechoulam, A.M. Zimmerman, S. Zimmerman, Proc. Natl. Acad. Sci. USA 91 (1994) 7678–7682.
[8] L. Venance, D. Piomelli, J. Glowinski, C. Giaume, Nature 376 (1995) 590–594.
[9] M. Sugita, M. Williams, J.T. Dulaney, H.W. Moser, Biochim. Biophys. Acta 398 (1975) 125–131.
[10] L. Facci, R. Dal Toso, S. Romanello, A. Buriani, S.D. Skaper, A. Leon, Proc. Natl. Acad. Sci. USA 92 (1995) 3376–3380.
[11] K.D. Chapman, S. Tripathy, B. Venables, A.D. Desouza, Plant Physiol. 116 (1998) 1163–1168.
[12] J.C. Domingo, M. Mora, M.A. de Madariaga, Biochim. Biophys. Acta 1148 (1993) 308–316.
[13] M. Mercadal, J.C. Domingo, M. Bermudez, M. Mora, M.A. De Madariaga, Biochim. Biophys. Acta 1235 (1995) 281–288.
[14] A. Ambrosini, E. Bertoli, P. Mariani, F. Tanfani, M. Wozniak, G. Zolese, Biochim. Biophys. Acta 1148 (1993) 351–355.
[15] M. Ramakrishnan, V. Sheeba, S.S. Komath, M.J. Swamy, Biochim. Biophys. Acta 1329 (1997) 302–310.
[16] M. Ramakrishnan, M.J. Swamy, Chem. Phys. Lipids 94 (1998) 43–51.
[17] M.J. Swamy, D. Marsh, M. Ramakrishnan, Biophys. J. 71 (1997) 2556–2564.
[18] S. Akoka, C. Tellier, C. LeRoux, D. Marion, Chem. Phys. Lipids 46 (1988) 43–50.
[19] S.R. Hall, G.S.D. King, J.M. Stewart (Eds.), Xtal 3.4 User's Manual, University of Western Australia, Perth, Australia, 1995.
[20] G.M. Sheldrick, SHELXL97. Program for the refinement of crystal structures, University of Göttingen, Göttingen, Germany, 1997.
[21] K. Larsson, in: F.D. Gunstone, J.L. Harwood, F.B. Padley (Eds.), The Lipid Handbook, Chapman and Hall, London, 1986, pp. 321–384.
[22] H. Hauser, I. Pascher, S. Sundell, J. Mol. Biol. 137 (1980) 249–263.
[23] K. Larsson, Acta Crystallogr. 21 (1966) 267–272.
[24] M. Goto, T. Takiguchi, Bull. Chem. Soc. Jpn. 58 (1985) 1319–1320.
[25] M. Goto, K. Kozawa, T. Uchida, Bull. Chem. Soc. Jpn. 61 (1988) 1434–1436.
[26] I. Pascher, M. Lundmark, P. Nyholm, S. Sundell, Biochim. Biophys. Acta 1113 (1992) 339–372.
[27] I. Pascher, S. Sundell, Chem. Phys. Lipids 37 (1985) 241–250.
[28] I. Pascher, S. Sundell, H. Hauser, J. Mol. Biol. 153 (1981) 807–824.